

Accepted Manuscript

Title: Highly Efficient C–Cl Bond Cleavage and Unprecedented C–C Bond Cleavage of Environmentally Toxic DDT through Molecular Electrochemical Catalysis

Authors: Xu Liang, Tingting Huang, Minzhi Li, John Mack, Martijn Wildervanck, Tebello Nyokong, Weihua Zhu



PII: S0926-860X(17)30336-8
DOI: <http://dx.doi.org/doi:10.1016/j.apcata.2017.07.026>
Reference: APCATA 16331

To appear in: *Applied Catalysis A: General*

Received date: 22-1-2017
Revised date: 3-7-2017
Accepted date: 15-7-2017

Please cite this article as: Xu Liang, Tingting Huang, Minzhi Li, John Mack, Martijn Wildervanck, Tebello Nyokong, Weihua Zhu, Highly Efficient C–Cl Bond Cleavage and Unprecedented C–C Bond Cleavage of Environmentally Toxic DDT through Molecular Electrochemical Catalysis, *Applied Catalysis A, General* <http://dx.doi.org/10.1016/j.apcata.2017.07.026>

This is a PDF file of an unedited manuscript that has been accepted for publication. As a service to our customers we are providing this early version of the manuscript. The manuscript will undergo copyediting, typesetting, and review of the resulting proof before it is published in its final form. Please note that during the production process errors may be discovered which could affect the content, and all legal disclaimers that apply to the journal pertain.

Highly Efficient C–Cl Bond Cleavage and Unprecedented C–C Bond Cleavage of Environmentally Toxic DDT through Molecular Electrochemical Catalysis

Xu Liang^{*,a}, Tingting Huang,^a Minzhi Li,^a John Mack^{*,b}, Martijn Wildervanck,^b Tebello Nyokong,^b and Weihua Zhu^{*,a}

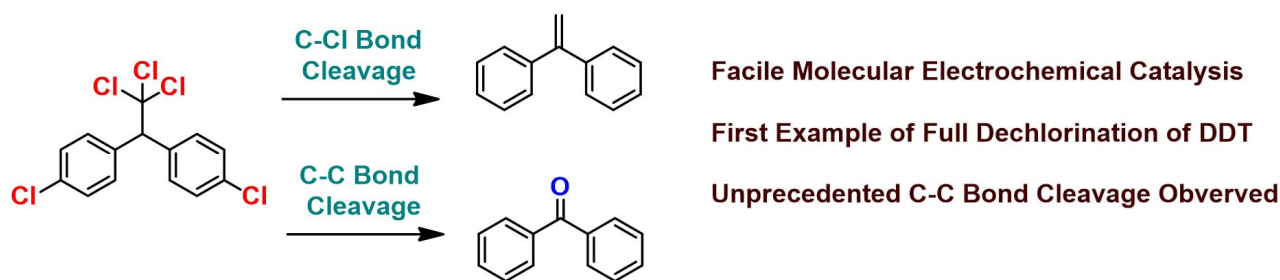
^aSchool of Chemistry and Chemical Engineering, Jiangsu University, Zhenjiang 212013, P. R. China;

^bDepartment of Chemistry, Rhodes University, Grahamstown 6140, South Africa

Corresponding Author

*E-mail: liangxu@ujs.edu.cn, Tel&Fax: +86-511-8879-1928 (to X.L.); E-mail: sayman@ujs.edu.cn, Tel&Fax: +86-511-8879-1928 (to W.Z.); E-mail: j.mack@ru.ac.za, Tel&Fax: +27-46-603-7234 (to J.M).

Graphical abstract



ABSTRACT

The electrocatalytic properties of a Co(II)octaalkoxyphthalocyanine complex (Co(II)Pc) with eight strongly electron-donating substituents provide the first example of the complete dechlorination of DDT through molecular electrocatalysis, rather than the use of metal electrodes which had been achieved previously. Interaction with a highly nucleophilic [Co(I)Pc]²⁻ species results in rapid cleavage of the C_(sp³)-Cl, C_(sp²)-Cl and aromatic C_(sp²)-Cl bonds. Bis(*p*-chlorophenyl)methanone (BPCl₂) is detected in high yield along with its full dechlorination product, diphenylmethanone (BP) and the conventional C–Cl bond cleavage products, due to an unprecedented C–C bond cleavage reaction that is followed by the formation of a C–O bond. Theoretical calculations are used to analyze trends in the electronic structure of the Co(II)octaalkoxyphthalocyanine complex that account for the efficiency of the C–Cl bond cleavage reactions, and the reaction process and mechanism are analyzed in depth.

KEYWORDS. C-Cl Bond Cleavage, C-C Bond Cleavage, Electrocatalysis, Phthalocyanine, Electronic Structure.

1. Introduction

Over the past few decades, organochlorides, organic compounds with at least one covalent C–Cl bond, such as 1,1-bis(4-chlorophenyl)-2,2,2-trichloroethane (DDT), pentachlorophenol (PCP), polychlorinated biphenyls (PCBs) and hexachlorocyclohexane (HCH) have been used in a wide range of applications [1-4]. Unfortunately, organochlorides often do not degrade in the environment, so despite restrictions being placed on their use in agriculture in many countries, they are still present around the world at significant concentrations as a ubiquitous contaminant in soils and waters [5-8]. There has been considerable interest in the development of new techniques to achieve their full degradation through C–Cl bond cleavage reactions. This has included microbial methods [9-14], along with chemical [15-19], photochemical [20-25] and electrochemical approaches [26-31].

There has been considerable interest in electrocatalytic processes due to their facile procedures and low cost. Electrocatalysis usually makes use of macrocyclic transition metal complexes, such as phthalocyanines (Pcs), porphyrins and cycloamines [32,33]. Typically, when a phthalocyanine is used, a central divalent metal ion is reduced electrochemically to form a $[M^I Pc(-2)]^-$ species, so it can react with alkyl halides (R–X) to form a σ -bond and a M^{III} -macrocycle, since this results in the release of a chloride ion through the cleavage of a C–Cl bond [34,35]. The dissociation energy of the bond is determined by the type of s-p hybridization that is involved. The values for $C_{(sp^3)}-Cl$ bonds lie in the 330–350 kJ/mol range, whereas those of $C_{(sp^2)}-Cl$ and aromatic $C_{(sp^2)}-Cl$ bonds lie in the 370–390 kJ/mol range and close to 400 kJ/mol, respectively [36-42]. The efficiency of C–Cl bond cleavage reactions differs significantly, therefore. For example, when iron(III)porphyrins were used as electroreductive catalysts for the dechlorination of lindane, pentachlorocyclohexene (PCCH), tetrachlorocyclohexadienes (TCDNs) and trichlorobenzenes (TCBs) were formed through the activation of the $C_{(sp^3)}-Cl$ bond, but there was no significant degradation of the more stable aromatic $C_{(sp^2)}-Cl$ bonds of the trichlorobenzenes [22,24].

One main challenge for researchers active in the field of electrocatalysis is to develop catalysts that can enable the complete dechlorination of environmentally problematic organochlorides, such as DDT. When Co^{II} , Fe^{III} and Mn^{III} porphyrins and Co^{II} phthalocyanines have previously been used as electrocatalysts, DDT has been degraded to form 1,1-bis(4-chlorophenyl)-2,2-dichloroethane (DDD), (1,1-bis(4-chlorophenyl)-2,2-dichloroethylene) (DDE), and (1,1-bis(4-chlorophenyl)-2-chloroethylene) (DDMU) since full $C_{(sp^3)}-Cl$ bond cleavage occurs followed by partial cleavage of the $C_{(sp^2)}-Cl$ bonds [20,21,23]. Although Ni^{II} salen complexes have been reported to enhance the dechlorination process, the activation yield for the $C_{(sp^2)}-Cl$ bond is still relatively low [43]. In this study, an electron-rich $Co(II)$ phthalocyanine (**1**) with eight electron-donating alkoxy substituents, $Co(II)-\alpha,\alpha'-(OC_5H_{11})_8Pc$, is used to provide the complete dechlorination of DDT in controlled-potential bulk electrolysis experiments. To the best of our knowledge, there have

previously been no reports of the full carbon-chlorine bond cleavage of DDT through molecular electrochemical catalysis, although this has been achieved previously with metal electrodes.

2. Experimental

2.1 Instrumentation

Bruker AVANCE 500 (500.13 MHz) or Bruker AVANCE 400 (400.03 MHz) spectrometers were used to measure ^1H NMR spectra. Residual solvent peaks were used to provide internal references for ^1H ($\delta = 7.26$ ppm for CDCl_3 , $\delta = 5.32$ ppm for CD_2Cl_2). Reagent grade chemicals and solvents were used as supplied unless otherwise noted. A three-electrode cell attached to a Chi-730D electrochemistry station was used during cyclic voltammetry measurements. A saturated calomel electrode (SCE), a glassy carbon disk, a platinum wire were the reference, working and counter electrodes, respectively. Bulk electrolysis was carried out with platinum mesh working and counter electrodes in an "H" type cell. The anodic and cathodic sections of the cell were separated with fritted glass and an SCE was used as the reference electrode and was placed in the same compartment as the working electrode. An optically transparent thin-layer cell with a Pt mesh working electrode that was assembled in house was attached to a Chi-730D potentiostat to enable the UV-visible spectroelectrochemical measurements. UV-visible spectra were recorded with a HP 8453A diode array spectrophotometer. A nitrogen atmosphere was used for all of the measurements that are related to electrochemistry and spectroelectrochemistry. Products of the electrolyses were identified with an Agilent HP6890 GC gas chromatography system equipped with a HP5975-MSD detector. A JASCO J-815 spectrodichromometer with a JASCO electromagnet (1.6 tesla) mounted in the sample compartment were used to record magnetic circular dichroism (MCD) spectra. Parallel and antiparallel fields were used and the intensity mechanism conventions that were recommended by Piepho and Schatz are used throughout [44-46].

2.2. Removal of supporting electrolyte

A pre-treatment procedure was required prior to the GC-MS measurements to remove the TBAP supporting electrolyte. The DMF solvent was evaporated under vacuum at 45°C on a rotary evaporator. Cyclohexane was then added to extract DDT and the dechlorinated products from the residue. The TBAP was removed after stirring and centrifuging, prior to the GC-MS analysis on HP6890-GC and HP5975-MSD systems with an HP-5 5% phenyl methyl siloxane column (length 30 m, ID 250 μm , film 0.25 μm). The temperature was initially set at 100°C and was then programmed to rise at $15^\circ\text{C}/\text{min}$ until a maximum of 300°C was reached. The intensity of the peaks was analyzed by area-normalized method. When the molar response factor for DDT was set as 1.00, the relative values for DDE, DDD and DDMU were determined to be 1.076 ± 0.039 , 0.934 ± 0.053 , 1.003 ± 0.031 , respectively. The molar response factors of some of the intermediate products could not be determined, since the appropriate reagent is not commercially available.

2.3. Computational methods

Geometry optimizations for unsubstituted metal free phthalocyanine (H_2Pc) and ethoxy-substituted model complexes for **1** and H_2 -**1** were carried out at the B3LYP/6-31G(d) level of theory by using the Gaussian 09 software package [47]. Slightly saddled structures were predicted with N–M–N angles in the central cavity of below 10° for **1**. The CAM-B3LYP functional was used for TD-DFT calculations, since it introduces a long-range correction at high interelectronic separations that makes it better suited for compounds and complexes that have excited states with significant charge transfer character.

2.4. Synthesis and Characterizations

2.4.1. Synthesis of 1,4-*n*-OC₅H₁₁-2,3-phthalonitrile. 1,4-(OH)₂-2,3-phthalonitrile (1.6 g, 10 mmol) was added to 20 mL of a dry acetone solution containing 1-iodopentane (4.4 g, 22 mmol, 2.2 eq.) and K₂CO₃ (5.5 g, 40 mmol, 4.0 eq). The resulting mixture was gradually heated to 60°C, and the temperature was maintained for 4 h. After removal of the solvent, the reaction mixture was purified by silica gel column chromatography with CHCl₃ as the eluent. Recrystallization from CHCl₃ and MeOH provided 1,4-*n*-OC₅H₁₁-2,3-phthalonitrile as a white solid compound in 88% yield (2.64 g). ¹H NMR (400 MHz, CDCl₃): δ = 7.15 (s, 2H; β -phenyl), 4.04 (t, J = 8.0 Hz, 4H; -OCH₂-), 1.84 (dd, J_1 =12.0 Hz, J_2 = 8.0 Hz, 4H; -CH₂-), 1.49–1.35 (m, 8H, -CH₂CH₂-), 0.93 (t, J = 8.0 Hz, 6H; -CH₃).

2.4.2. Synthesis of H₂- α,α' -*n*-(OC₅H₁₁)₈-phthalocyanine (1-H₂**):** lithium (56 mg, 8.0 mmol) was added to 6 mL of freshly distilled 1-butanol, and the solution was stirred and heated at 150°C under an N₂ atmosphere until the lithium was completely dissolved. 1,4-OC₅H₁₁-2,3-phthalonitrile (300 mg, 1.0 mmol) was then added and the resulting mixture was gradually heated at 60°C, and the temperature was maintained for 2 h. After removal of the solvent, the reaction mixture was purified by silica gel column chromatography with CHCl₃:MeOH (100:3) as the eluent. Recrystallization from CHCl₃ and MeOH provided the target compound, **2**, as a green solid in 63% yield (2.64 g). ¹H NMR (400 MHz, CDCl₃): δ = 7.15 (s, 2H; β -phenyl), 4.04 (t, J = 8.0 Hz, 4H; -OCH₂-), 1.84 (dd, J_1 =12.0 Hz, J_2 = 8.0 Hz, 4H; -CH₂-), 1.49–1.35 (m, 8H, -CH₂CH₂-), 0.93 (t, J = 8.0 Hz, 6H; -CH₃). MALDI-TOF-MS: m/z = 1203.83 (Calcd. for C₇₂H₉₈N₈O₈ [M]⁺ = 1203.60).

2.4.3. Synthesis of Co(II)- α,α' -*n*-(OC₅H₁₁)₈Pc (1**).** Co(CH₃COO)₂·4H₂O (100 mg, 4.0 mmol, 4.0 eq) and H₂Pc (120 mg, 1.0 mmol) were dissolved in 4 mL of anhydrous DMF, stirred and heated at 180°C for 20 min under N₂. The reaction mixture was poured into 30 mL of ice-water once it had cooled to room temperature. After filtration, a green solid was collected and further purified by alumina gel column chromatography with CHCl₃:MeOH (100:5) as the eluent. The target compound **3b** was obtained in 90% yield. MALDI-TOF-MS: m/z = 1260.73 (Calcd. for C₇₂H₉₈N₈O₈ [M]⁺ = 1260.51).

3. Results and Discussion

3.1 Synthesis of the molecular catalyst

The literature procedure was used to prepare **1** [48], with a CoCl₂ salt used during the metal insertion step (**Scheme 1**). Trends that are identified in the electronic structures and optical properties of metal phthalocyanine complexes can be used to rationalize their redox and

electrocatalytic properties [49-53].

3.2. Spectroscopic investigation and theoretical calculation

A perimeter model approach can be used to analyze trends in the electronic structures of porphyrinoid metal complexes [49-56], by considering the effect that structural modifications perturbations have on the frontier molecular orbitals (MOs) of a D_{16h} symmetry $C_{16}H_{16}^{2-}$ parent perimeter that corresponds to the inner perimeter of the ligand. There is a $M_L = 0, \pm 1, \pm 2, \pm 3, \pm 4, \pm 5, \pm 6, \pm 7, 8$ sequence in the π -MOs of the $C_{16}H_{16}^{2-}$. The HOMO and LUMO have M_L values of ± 4 and ± 5 , respectively. This forms the basis of Gouterman's 4-orbital model [57], which is comprised of a forbidden lower energy Q ($\Delta M_L = \pm 9$) transition and an allowed B ($\Delta M_L = \pm 1$) transition at higher energy. Spectral band deconvolution analyses have demonstrated that two intense overlapping B_1 and B_2 bands are present in the B band region of phthalocyanine spectra, due to configurational interaction with π -MOs that are associated with the peripheral fused benzene rings [58-60]. Michl [51-55] introduced a terminology in which π -MOs derived from the HOMO and LUMO of the parent $C_{16}H_{16}^{2-}$ species that have an angular node aligned with the y -axis as the **a** and **-a MOs**, respectively, whereas analogous MOs that lie on antinodes are referred to as the **s** and **-s MOs** (Fig. 2), since this facilitates a comparison of porphyrinoid derivatives of different symmetry, such as **1** and H_2 -**1**.

Derivative-shaped Faraday **A**₁ terms dominate the MCD spectra of metal phthalocyanine complexes, such as **1**, that have a four-fold axis of symmetry, since the excited states are orbitally degenerate [44-46,54-56]. When the symmetry of the phthalocyanine ligand is lowered so there is no three-fold or higher symmetry axis, as is the case with the free base ligand of **1** (H_2 -**1**), coupled pairs of Gaussian-shaped oppositely-signed **B**₀ terms become the dominant spectral feature. Since the **A**₁ term at 735 nm in the spectrum of **1** corresponds to the absorption band at 738 nm, this band can be readily assigned to the Q transition. In a similar manner, the **A**₁ term and absorption band at 322 nm can be assigned to the B transition, slightly to the red of where they are predicted to lie in the TD-DFT calculation (Fig. 1). Metal-to-ligand charge-transfer bands of **1** are predicted to lie to the red of the Q band, and other charge-transfer bands are predicted in the B band region (Figs. 1 and 2). There is a relative destabilization of the **a** MO (the HOMO), because there are larger MO coefficients at the non-peripheral positions on the fused benzene rings than is the case with the **s**, **-a** and **-s** MOs. This leads to a narrowing of the HOMO-LUMO gap of H_2 -**1** relative to the parent unsubstituted H_2 Pc (Fig. 2), and explains why the Q bands are red-shifted to beyond 700 nm (Fig. 1). The blue shift of the Q band of **1** compared to those of H_2 -**1** (Fig. 1) is related to mixing between the LUMO of the Pc π -system (Fig. 2) and the occupied $3d_{xz}$ and $3d_{yz}$ ($3d_{\pi}$) orbitals for symmetry systems [57].

3.3. Electrochemical measurements

Electrochemical measurements were carried out in DMF to provide further insight into the electronic properties of **1**, since it is well established that the HOMO and LUMO energies of

phthalocyanine derivatives correlate closely with their first oxidation and reduction potentials when the central metal is not electroactive [46,61-65]. The electron-donating alkoxy substituents were expected to increase the electron density on the phthalocyanine π -system, which leads to more difficult reduction and easier oxidation, and hence in the formation of stronger reducing agents when reduced anionic species are formed. The cyclic voltammograms of **1** contain two reversible oxidation steps at +0.54 and +0.91 V, and two reversible reduction processes at -0.42 and -1.53 V that can be assigned, respectively, to metal-centered reduction $[\text{Co}^{\text{II}}\text{Pc}(-2)]/[\text{Co}^{\text{I}}\text{Pc}(-2)]^-$ and π -anion formation $[\text{Co}^{\text{I}}\text{Pc}(-2)]^-/[\text{Co}^{\text{I}}\text{Pc}(-3)]^{2-}$ steps [66-69]. Additional irreversible reduction peaks are observed following the $[\text{Co}^{\text{II}}\text{Pc}(-2)]/[\text{Co}^{\text{I}}\text{Pc}(-2)]^-$ reduction step upon addition of 0.0–2.0 eq of DDT as indicated by an asterisk in the cyclic voltammograms (Fig 3, left), which can be assigned to irreversible reductions of one or more of the σ -bonded $[\text{Co}^{\text{III}}\text{Pc}(-2)]^+$ species that are generated from the reaction between $[\text{Co}^{\text{I}}\text{Pc}(-2)]^-$ and DDT. The irreversible peak potentials are about 500–600 mV more negative than the reversible $[\text{Co}^{\text{II}}\text{Pc}(-2)]/[\text{Co}^{\text{I}}\text{Pc}(-2)]^-$ step at -0.42 V. The increase in the cathodic peak current for the $[\text{Co}^{\text{I}}\text{Pc}(-2)]^-/[\text{Co}^{\text{I}}\text{Pc}(-3)]^{2-}$ process upon addition of DDT is more significant than for the $[\text{Co}^{\text{II}}\text{Pc}(-2)]/[\text{Co}^{\text{I}}\text{Pc}(-2)]^-$ process (Fig. 3, right). This indicates that the reactivity of the $[\text{Co}^{\text{I}}\text{Pc}(-3)]^{2-}$ species towards DDT is significantly higher.

3.4. Spectroelectrochemical measurements

Spectroelectrochemistry can be used to monitor the chemical reactions between reduced metalloporphyrinoids and organochlorides, which produce metal-carbon bond derivatives as the key intermediates [70-72]. The spectral changes which occur during the first two reduction steps of **1** in the absence and presence of DDT are shown in Fig. 4. Identical spectral changes are observed during the first one-electron reduction step in the presence and absence of DDT. When the potential was set at $E = -1.80$ V, the spectral changes in the absence of DDT exhibits a decrease of the absorption intensity in both B and Q band regions, along with an increase in the intensity of the absorption bands at 463 and 578 nm, which is characteristic of the formation of a $[\text{Co}^{\text{I}}\text{Pc}(-3)]^{2-}$ species [73,74]. After 5.0 eq of DDT is added, significant differences are clearly observed. The final UV-visible absorption spectrum displays similar decreases in the intensity in the B and Q band regions, with increased absorbance observed in the visible region. This is consistent with the cyclic voltammetric properties, since a catalytic reaction involving DDT and the electrogenerated $[\text{Co}^{\text{I}}\text{Pc}(-3)]^{2-}$ species occurs after the second reduction step. Controlled-potential bulk electrolyses were carried out in 2.0×10^{-4} M DMF solutions of **1**, 0.1 M TBAP, 15.0 eq of DDT (3.0×10^{-3} M) and 50 μL of trimethylamine, in order to determine the C–Cl bond cleavage products during electrocatalysis. The bulk electrolysis potential was set at $E = -1.85$ V, which is sufficient to generate the doubly reduced $[\text{Co}^{\text{I}}\text{Pc}(-3)]^{2-}$ species and also to reduce the homogeneously generated σ -bonded $\text{Co}^{\text{III}}\text{Pc}$ intermediates. Since decomposition components of the TBAP supporting electrolyte are formed during high temperature gas chromatography (GC), it was necessary to first remove the supporting electrolyte to prevent blockage of the column by following procedures described in the experimental section.

3.5 Electrochemical catalyzed carbon-chlorine bond cleavage

According to previously reported electrocatalysis results [23], the C–Cl bond cleavage of DDT is initially achieved through $C_{(sp^3)}$ –Cl bond cleavage with a roughly 1:1 ratio in the formation of (1,1-bis(4-chlorophenyl)-2,2-dichloroethane) (DDD) and (1,1-bis(4-chlorophenyl)-2,2-dichloroethylene) (DDE). Subsequently, (1,1-bis(4-chlorophenyl)-2-chloroethylene) (DDMU) is slowly formed through $C_{(sp^3)}$ –Cl bond cleavage of DDD or $C_{(sp^2)}$ –Cl bond cleavage of DDE. DDMU is usually the main ultimate degradation product with only trace amounts of further C–Cl bond cleavage products being formed, due to the low reactivity of the highly stable $C_{(sp^2)}$ –Cl and aromatic $C_{(sp^2)}$ –Cl bonds. In contrast, when **1** is used as a catalyst, the initial $C_{(sp^3)}$ –Cl bond cleavage reaction is extremely fast and DDE is obtained with high selectivity (Fig. 5 and Scheme 2). DDE is subsequently completely converted to DDMU through $C_{(sp^2)}$ –Cl bond cleavage. The further $C_{(sp^2)}$ –Cl bond cleavage of DDMU was fully complete within 4 h and yields dichlorophenylethylene (DPECl₂) and its stable aromatic $C_{(sp^2)}$ –Cl bond cleavage products (Fig. 5, middle). This C–Cl bond cleavage system provides the most satisfactory result that has been reported to date for DDT dechlorination, since the reaction does not stop at the DDMU step. After electrolysis for 6 h, all of the products containing even a single aromatic $C_{(sp^2)}$ –Cl bond were completely degraded. Diphenylethylene (DPE), the full dechlorination product of DDT, was obtained for the first time (**Scheme 2**) and DPE was completely reduced to diphenylethane (DPEA) in ca. 57% yield. The obvious explanation for this is that the incorporation of electron-rich alkoxy groups at the non-peripheral positions results in an unusually electron-rich Pc ligand and hence forms a very strong reducing agent during electrocatalysis, since there is a significant interaction between the LUMO of the phthalocyanine π -system and the $3d_{xz}$ and $3d_{yz}$ orbitals of the central Co(II) ion (Fig. 2) [57].

Surprisingly, when **1** is used as the catalyst in DMF, products resulting from C–C bond cleavage reactions are also observed (Fig. 5, right). The formation of dichlorophenylmethane (DPM) can readily be explained, since the key intermediate, dichlorophenylcarbon anion, reacts with water during the quenching of the reaction (Scheme 3). When heavy water (D₂O) was used deuterated dichlorophenylmethane-*d* (DPM-*d*) was identified by GC-MS analysis. The formation of *p,p'*-dichlorobenzophenone (BPCl₂) as a C–O bond formation product probably results from a reaction between the *p,p'*-dichlorophenylcarbon anion and oxygen gas, since trace levels of oxygen gas may enter from the working electrode compartment or may be present as a trace impurity in the nitrogen gas that is used during the electrolysis. The C–C bond cleavage reaction is a rapid one, whereas the C–O formation occurs on a longer timescale. It is noteworthy that *p*-chlorobenzophenone (BPCl) and benzophenone (BP), the partial and full C–Cl bond cleavage products for *p,p'*-dichlorobenzophenone (BPCl₂) (Scheme 2), were also obtained in significant yields. The use of Co(II)- α,α' -(OC₅H₁₁)₈Pc, as a catalyst for the electroreduction of DDT, results in highly efficient C–Cl bond cleavage and provides the first example of the full dechlorination of DDT through molecular electrochemical catalysis. It should be emphasized, however, that similar results

for the electroreduction of carbon-halide bonds have recently reported by Gennaro et al. through the use of a silver cathode [75] and that the complete dechlorination of DDT had already been achieved previously through the use of other metal electrodes [19,31,76]. GC-MS analysis identified the formation in high yield of bis(*p*-chlorophenyl)methanone (BPCl₂), along with diphenylmethanone (BP) upon full dechlorination, due to C–C bond cleavage followed by C–O bond formation, which has not been reported previously during the electrocatalysis of DDT. The highly efficient C–Cl bond cleavage reported in this study has a broad range of potential applications in both chemistry and environmental remediation.

3.6. Reaction process and mechanism study

To confirm the reaction process and the mechanisms for the C–Cl and C–C bond cleavages, electrochemical and spectroelectrochemical measurements and controlled-potential bulk electrolyses of DDD, DDE and DDMU were carried out in the presence of **1** under identical conditions. There are significant differences in the electrochemical measurements upon addition of 0 – 2 eq of DDD, DDE and DDMU, Fig. 6. Irreversible reduction peaks are observed following the [Co^{II}Pc(–2)]/[Co^IPc(–2)][–] reduction step upon addition of DDD in DMF, but not for DDE and DDMU. This demonstrates that the carbon atom s-p hybridization of the C–Cl bond and the local environment of the chlorine atom significantly influence the electrochemical behavior, so the C–Cl bond cleavage process can be separated into a series of different reactions. When 5 eq of DDD, DDE and DDMU are added to solutions of **1** in DMF, the observed spectral changes (Fig. 7) of DDD are similar to those obtained with DDT, but those observed with DDE and DDMU are not. In the case of DDD, diagnostic decreases are observed in the B and Q band regions at $E = -1.85$ V, along with an increase in absorbance at 470 nm. In contrast, for DDE and DDMU, an increase in intensity at 572 nm was observed. This indicates that cleavage of the C_(sp³)–Cl and C_(sp²)–Cl bonds of DDT can be readily distinguished by spectroelectrochemical measurements. Time-dependent GC analysis of the controlled-potential bulk electrolysis of DDE (Fig. 8) demonstrates that a C_(sp²)–Cl bond cleavage reaction initially yields DDMU, and then an aromatic C_(sp²)–Cl bond cleavage forms DPECl₂, DPECl and DPE (Scheme 2), which in turn are converted to diphenylethane (DPEA) in approximately the same ratio as that observed during the electrolysis of DDT. At the same time, the C–C bond cleavage process also results in the formation of chlorobenzophenone and benzophenone (BP). In the case of DDMU (Fig. 9), the time-dependent changes in the C–Cl bond cleavage reaction products are quite similar to those for DDT and DDE with the final conversion to DPEA occurring within a shorter time, but in contrast the final product yields for C–C bond cleavage decrease significantly to less than 4.0%. This can be readily explained, since DDMU is less electronegative due to the lower number of chlorine atoms, making the initial nucleophilic attack more difficult. These results confirm that the C–C bond cleavage reaction mainly occurs due to the C–Cl bond cleavage of DDE, and are consistent with the proposed mechanism for the C–Cl bond cleavage of DDT (Scheme 2). On the other hand, both C–Cl and C–C bond cleavage products were observed in the case of DDD (Fig. 10), but there is a significant difference in the product

distributions. Since the fraction of DDD formation is relatively small, the influence of DDD in this system can usually be omitted from consideration.

4. Conclusions

In summary, the use of an electron-rich cobalt(II)phthalocyanine, Co(II)- α,α' -(OC₅H₁₁)₈Pc, as a catalyst for the electroreduction of DDT, results in highly efficient C–Cl bond cleavage and provides the first example of the full dechlorination of DDT through molecular electrochemical catalysis, rather than the use of metal electrodes which had been achieved previously. Time-dependent GC analyses have been used to identify the degradation products so that the reaction kinetics and mechanism can be studied in detail. This identified the formation in high yield of *bis*(*p*-chlorophenyl)methanone (BPCl₂), along with diphenylmethanone (BP) upon full dechlorination, due to C–C bond cleavage followed by C–O bond formation, which has previously not been reported during the electrocatalytic reduction of DDT. The incorporation of electron-rich alkoxy groups at the non-peripheral positions results in an unusually electron-rich Pc ligand and hence forms a very strong reducing agent during electrocatalysis, since there is a significant interaction between the LUMO of the π -system and the 3d orbitals of the central metal ion. The highly efficient C–Cl bond cleavage reported in this study has a broad range of potential applications in both chemistry and environmental science. This study should also provide information that helps to guide rational design of other porphyrinoid complexes that are suitable for use as electrocatalysts in organic synthesis and in the remediation of environmentally problematic organochlorides.

Supplementary Material. Details of the TD-DFT calculations are provided.

Acknowledgements

Financial support in China were provided by National Natural Science Foundation of China (No. 21171076), Natural Science Foundation of Jiangsu Province, P. R. China (No. BK200160449) to X. L. and W. Z., and NRF of South Africa CSUR grant (uid: 93627) to JM. The theoretical calculations were carried out at the Centre for High Performance Computing in Cape Town.

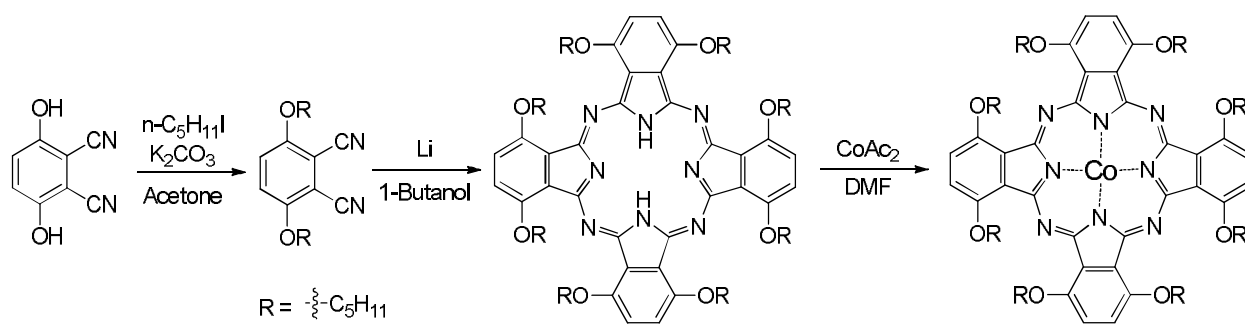
References

- [1] A.L. Chiuchiolo, R.M. Dickhut, M.A. Cochran, H.W. Ducklow, *Environ. Sci. Technol.* 38 (2004) 3551–3557.
- [2] F. Rigas, K. Papadopoulou, V. Dritsa, D. Doulia, *J. Hazard. Mater.* 140 (2007) 325–332.
- [3] B.C. Okeke, T. Siddique, M.C. Arbestain, W.T. Frankenberger, *J. Agric. Food Chem.* 50 (2002) 2548–2555.
- [4] H.L. Beasley, T. Phongkham, M.H. Daunt, S.L. Guihot, J.H. Skerritt, *J. Agric. Food Chem.* 46 (1998) 3339–3352.
- [5] M. Arkas, R. Allabashi, D. Tsiourvas, E.M.R. Perfler, *Environ. Sci. Technol.* 40 (2006) 2771–2781.
- [6] L.S. Zhang, J.M. Ma, S. Venkatesh, Y.F. Li, P. Cheung, *Environ. Sci. Technol.* 42 (2008) 8791–8797.
- [7] T. Ali, E.A. Mehmet, A. Senar, T. Mustafa, B. Fatma, *J. Hazard. Mater.* 262 (2013) 656–663.
- [8] T.M. Phillips, A.G. Seech, H. Lee, J.T. Trevors, *J. Microbiol. Methods* 47 (2001) 181–188.
- [9] J.F. Quensen III, S.A. Mueller, M.K. Jain, J.M. Tiedje, *Science* 280 (1998) 722–724.
- [10] K. Ise, K. Suto, C. Inoue, *Environ. Sci. Technol.* 45 (2011) 5339–5345.
- [11] J.J. Pagano, R.J. Scudato, R.N. Roberts, J.C. Bemis, *Environ. Sci. Technol.* 29 (1995) 2584–2589.
- [12] F. Cao, F.B. Li, T.X. Liu, D.Y. Huang, C.Y. Wu, C.H. Feng, X.M. Li, *J. Agric. Food Chem.* 58 (2010) 12366–12372.
- [13] L.S. LaRoe, A.D. Fricker, D.L. Bedard, *Environ. Sci. Technol.* 48 (2014) 9187–9196.
- [14] S.L. Badea, C. Vogt, S. Weber, A.F. Danet, H.H. Richnow, *Environ. Sci. Technol.* 43 (2009) 3155–3161.
- [15] G.J. Su, H.J. Lu, L.X. Zhang, A.Q. Zhang, L.Y. Huang, S. Liu, L.W. Li, M.W. Zheng, *Environ. Sci. Technol.* 48 (2014) 6899–6908.
- [16] H.Y. Jeong, K.F. Hayes, *Environ. Sci. Technol.* 37 (2003) 4650–4655.
- [17] X.L. Ge, L. Shi, X. Wang, *Ind. Eng. Chem. Res.* 53 (2014) 6351–6357.
- [18] G.V. Lowry, K.M. Johnson, *Environ. Sci. Technol.* 38 (2004) 5208–5216.
- [19] G.D. Sayles, G.R. You, M.X. Wang, M.J. Kupferle, *Environ. Sci. Technol.* 31 (1997) 3448–3454.
- [20] M.Z. Li, L.L. Liang, C. Ni, X. Liang, W.H. Zhu, *J. Electroanal. Chem.* 766 (2016) 135–140.
- [21] J.G. Shao, A. Thomas, B.C. Han, C.A. Hansen, *J. Porphyrins Phthalocyanines* 14 (2010) 133–141.
- [22] W.H. Zhu, C. Ni, L.L. Liang, W.J. Li, M.Z. Li, Z.P. Ou, K.M. Kadish, *J. Porphyrins Phthalocyanines* 18 (2014) 519–527.
- [23] W.H. Zhu, Y.Y. Fang, W. Shen, G.F. Lu, Y. Zhang, Z.P. Ou, K.M. Kadish, *J. Porphyrins Phthalocyanines* 15 (2010) 66–74.
- [24] W.H. Zhu, T.T. Huang, M.F. Qin, M.Z. Li, J. Mack, X. Liang, *J. Electroanal. Chem.* 774 (2016) 58–65.
- [25] S.O. Obare, O.T. Ito, G.J. Meyer, *Environ. Sci. Technol.* 39 (2005) 6266–6272.
- [26] C.M. McGuire, D.G. Peters, *Electrochem. Acta* 137 (2014) 423–430.
- [27] A. Matsunaga, A. Yasuhara, *Chemosphere* 59 (2005) 1487–1496.
- [28] J.P. Merz, B.C. Gamoke, M.P. Foley, K. Raghavachari, D.G. Peters, *J. Electroanal. Chem.* 660 (2011) 121–126.

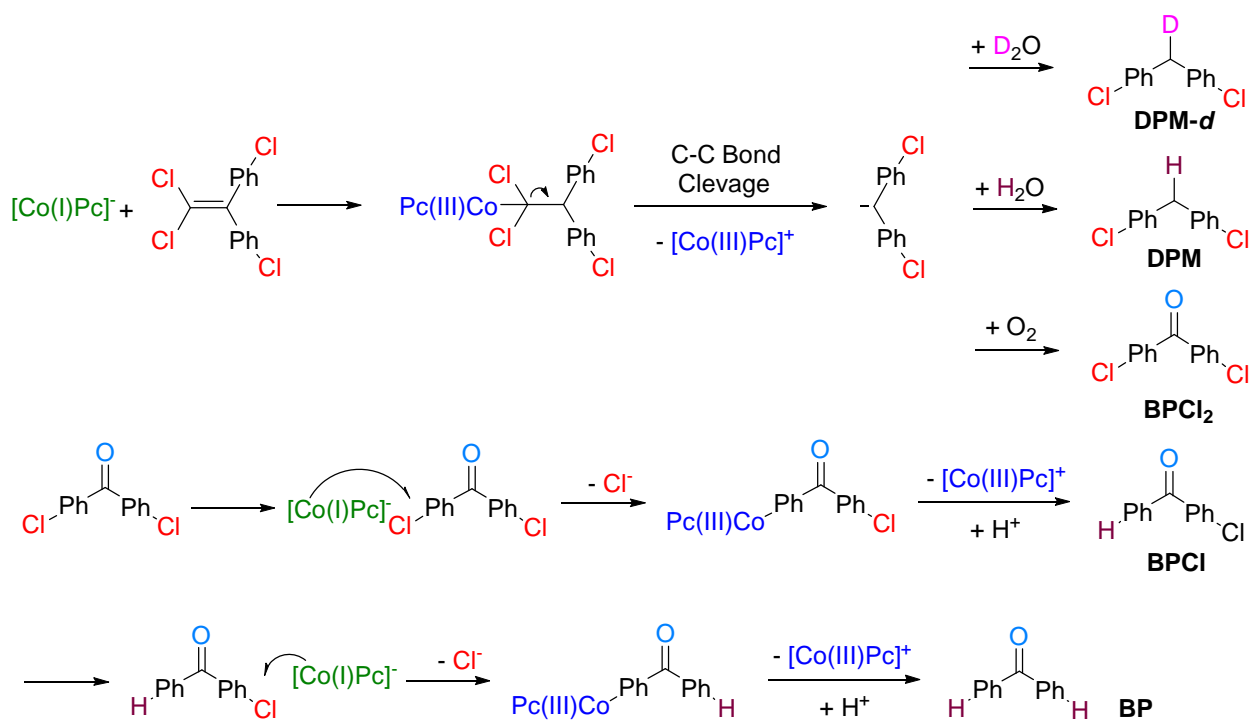
- [29] A.A. Peverly, J.K. Karty, D.G. Peters, *J. Electroanal. Chem.* 692 (2013) 66–71.
- [30] P.R. Birkin, A. Evans, C. Milhano, M.I. Montenegro, D. Pletcher, *Electroanalysis* 16 (2004) 583–587.
- [31] F. Alonso, I.P. Beletskaya, M. Yus, *Chem. Rev.* 102 (2002) 4009–4091.
- [32] L. Chen, E.A. Capanema, H.S. Grasz, *J. Agric. Food Chem.* 51 (2003) 1932–1941.
- [33] L. Chen, E.A. Capanema, H.S. Grasz, *J. Agric. Food Chem.* 51 (2003) 6223–6232.
- [34] K.M. Kadish, M.M. Franzen, B.C. Han, C. AraulloMcAdams, D. Sazou, *Inorg. Chem.* 31 (1992) 4399–4403.
- [35] G.B. Maiya, B.C. Han, K.M. Kadish, *Langmuir* 5 (1989) 645–650.
- [36] E.C.M. Chen, K. Albyn, L. Dussack, *J. Phys. Chem.* 93 (1989) 6827–6832.
- [37] A.F. Lago, T. Baer, *Int. J. Mass Spectrom.* 252 (2006) 20–25.
- [38] K. Miyokawa, E. Tschuikow-Roux, *J. Phys. Chem.* 94 (1990) 715–722.
- [39] J.A. Seetula, *J. Chem. Soc., Faraday Trans.* 92 (1996) 3069–3078.
- [40] L. Sheng, F. Qi, H. Gao, Y. Zhang, S. Yu, W.K. Li, *Int. J. Mass Spectrom.* 161 (1997) 151–159.
- [41] H.J. Wang, Y. Fu, C. Wang, Q.X. Guo, *Acta Chim. Sinica* 66 (2008) 362–370.
- [42] Y.M. Wang, C. Zhou, Y. Fu, L. Liu, Q.X. Guo, *Chin. J. Org. Chem.* 25 (2005) 1398–1402.
- [43] E.R. Wagoner, J.L. Hayes, J.A. Karty, D.G. Peters, *J. Electroanal. Chem.* 706 (2013) 55–63.
- [44] S.B. Piepho, P.N. Schatz, *Group Theory in Spectroscopy With Applications to Magnetic Circular Dichroism*, John Wiley&Sons, Hoboken, NJ, 1983.
- [45] N. Kobayashi, A. Muranaka, J. Mack, *Circular Dichroism and Magnetic Circular Dichroism Spectroscopy for Organic Chemists*, Royal Society of Chemistry, Cambridge, 2011.
- [46] J. Mack, N. Kobayashi, *Chem. Rev.* 111 (2011) 281–321.
- [47] M.J. Frisch, G.W. Trucks, H.B. Schlegel, G.E. Scuseria, M.A. Robb, J.R. Cheeseman, G. Scalmani, V. Barone, B. Mennucci, G.A. Petersson, H. Nakatsuji, M. Caricato, X. Li, H.P. Hratchian, A.F. Izmaylov, J. Bloino, G. Zheng, J.L. Sonnenberg, M. Hada, M. Ehara, K. Toyota, R. Fukuda, J. Hasegawa, M. Ishida, T. Nakajima, Y. Honda, O. Kitao, H. Nakai, T. Vreven, J.A. Montgomery, J.E. Peralta, F. Ogliaro, M. Bearpark, J.J. Heyd, E. Brothers, K.N. Kudin, V.N. Staroverov, R. Kobayashi, J. Normand, K. Raghavachari, A. Rendell, J.C. Burant, S.S. Iyengar, J. Tomasi, M. Cossi, N. Rega, M.J. Millam, M. Klene, J.E. Knox, J.B. Cross, V. Bakken, C. Adamo, J. Jaramillo, R. Gomperts, R.E. Stratmann, O. Yazyev, A.J. Austin, R. Cammi, C. Pomelli, J.W. Ochterski, R.L. Martin, K. Morokuma, V.G. Zakrzewski, G.A. Voth, P. Salvador, J.J. Dannenberg, S. Dapprich, A.D. Daniels, Ö. Farkas, J.B. Foresman, J.V. Ortiz, J. Cioslowski, D.J. Fox, *Gaussian 09, Revision D.01*, Gaussian, Inc., Wallingford, CT, 2009.
- [48] Y. Jiang, M.Z. Li, X. Liang, J. Mack, M. Wildervanck, T. Nyokong, M.F. Qin, W.H. Zhu, *Dalton Trans.* 44 (2015) 18237–18246.
- [49] W. Moffitt, *J. Chem. Phys.* 22 (1954) 320–333.
- [50] W. Moffitt, *J. Chem. Phys.* 22 (1954) 1820–1829.
- [51] J. Michl, *J. Am. Chem. Soc.* 100 (1978) 6801–6811.

- [52] J. Michl, *Pure Appl. Chem.* 52 (1980) 1549–1563.
- [53] J. Michl, *Tetrahedron* 40 (1984) 3845–3934.
- [54] J. Michl, *J. Am. Chem. Soc.* 100 (1978) 6812–6818.
- [55] J. Michl, *J. Am. Chem. Soc.* 100 (1978) 6819–6824.
- [56] J. Mack, Y. Asano, N. Kobayashi, M.J. Stillman, *J. Am. Chem. Soc.* 127 (2005) 17697–17711.
- [57] M. Gouterman, in: D. Dolphin (Ed.), *The Porphyrins*, vol. III, Part A, Academic Press, New York, 1978, pp. 1–165.
- [58] T. Nyokong, Z. Gasyana, M.J. Stillman, *Inorg. Chem.* 26 (1987) 548–553.
- [59] T. Nyokong, Z. Gasyana, M.J. Stillman, *Inorg. Chem.* 26 (1987) 1087–1095.
- [60] E.A. Ough, T. Nyokong, K.A.M. Creber, M.J. Stillman, *Inorg. Chem.* 27 (1988) 2724–2732.
- [61] R.J. Li, X.X. Zhang, P.H. Zhu, D.K.P. Ng, N. Kobayashi, J.Z. Jiang, *Inorg. Chem.* 45 (2006) 2327–2334.
- [62] N. Kobayashi, H. Miwa, V.N. Nemykin, *J. Am. Chem. Soc.* 124 (2002) 8007–8020.
- [63] B.Z. Yu, A.B.P. Lever, T.W. Swaddle, *Inorg. Chem.* 43 (2004) 4496–4504.
- [64] Y.Z. Bian, L. Li, J.M. Dou, D.Y. Cheng, R.J. Li, C.Q. Ma, D.K.P. Ng, N. Kobayashi, J.Z. Jiang, *Inorg. Chem.* 43 (2004) 7539–7544.
- [65] A.B.P. Lever, P.C. Minor, *Inorg. Chem.* 20 (1981) 4015–4017.
- [66] W.A. Nevin, M.R. Hempstead, W. Liu, C.C. Leznoff, A.B.P. Lever, *Inorg. Chem.* 26 (1987) 570–577.
P.J. Lukes, A.C. McGregor, T. Clifford, J.A. Crayston, *Inorg. Chem.* 31 (1992) 4697–4699.
- [67] W.A. Nevin, W. Liu, S. Greenberg, M.R. Hempstead, S.M. Marcuccio, M. Melnik, C.C. Leznoff, A.B.P. Lever, *Inorg. Chem.* 26 (1987) 891–899.
- [68] T.T. Tasso, T. Furuyama, N. Kobayashi, *Inorg. Chem.* 52 (2013) 9206–9215.
- [69] G.F. Mori, Z. Fu, E. Viola, X.H. Cai, C. Ercolani, M.P. Donzello, K.M. Kadish, *Inorg. Chem.* 50 (2011) 8225–8237.
- [70] K.M. Kadish, B.C. Han, A. Endo, *Inorg. Chem.* 30 (1991) 4502–4506.
- [71] D. Lexa, J. Mispelster, J.M. Saveant, *J. Am. Chem. Soc.* 103 (1981) 6806–6812.
- [72] J.G. Shao, J. Comodore, B.C. Han, C. Prunte, C.A. Hansen, *J. Porphyrins Phthalocyanines* 13 (2009) 876–887.
- [73] D.W. Clack, J.R. Yandle, *Inorg. Chem.* 11 (1972) 1738–1742.
- [74] J. Mack, M.J. Stillman, *Inorg. Chem.* 36 (1997) 413–425.
- [75] A. Gennaro, A.A. Isse, P. R. Mussini in: O. Hammerich, B. Speiser, (Eds.), *Organic Electrochemistry*, 5th Edition, CRC Press, Boca Raton, 2016, pp. 917–940.
- [76] M.D. Engelmann, J.G. Doyle, I.F. Cheng, *Chemosphere*, 43 (2001) 195–198.
- [77] Y. Ukisu, *J. Hazard. Mater.*, 152 (2008) 287–292.

Schemes



Scheme 1. Synthesis of Co(II)- α,α' -(OC₅H₁₁)₈Phthalocyanine **1**.



Scheme 3. Proposed C–C bond cleavage and C–O bond formation in DMF during the electrochemical reduction process with **1**.

Figures

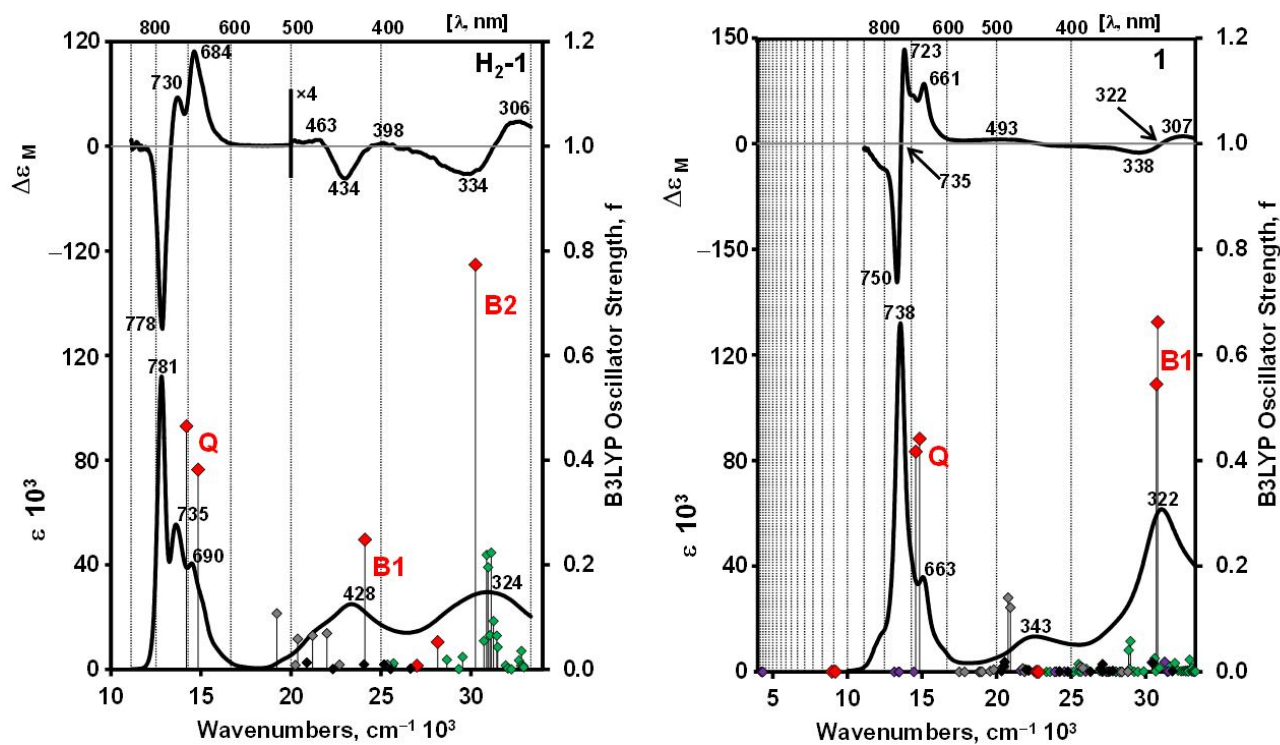


Fig. 1. Magnetic circular dichroism (TOP) and electronic absorption spectra (BOTTOM) of **1** (RIGHT) and its non-metallated precursor (H_2-1 , LEFT) in CH_2Cl_2 . A secondary axis is used for the TD-DFT spectra. The Q and B_1 bands that are associated with Gouterman's 4-orbital model [56] are highlighted with red diamonds. Smaller black, green, gray and purple diamonds are used to differentiate the $\pi\pi^*$ bands, the remaining $\pi\pi^*$ bands, bands that are associated with π -MOs that have large MO coefficients on the peripheral fused benzene rings, and transitions that are associated with the 3d MOs of the central Co(II) ion, respectively.

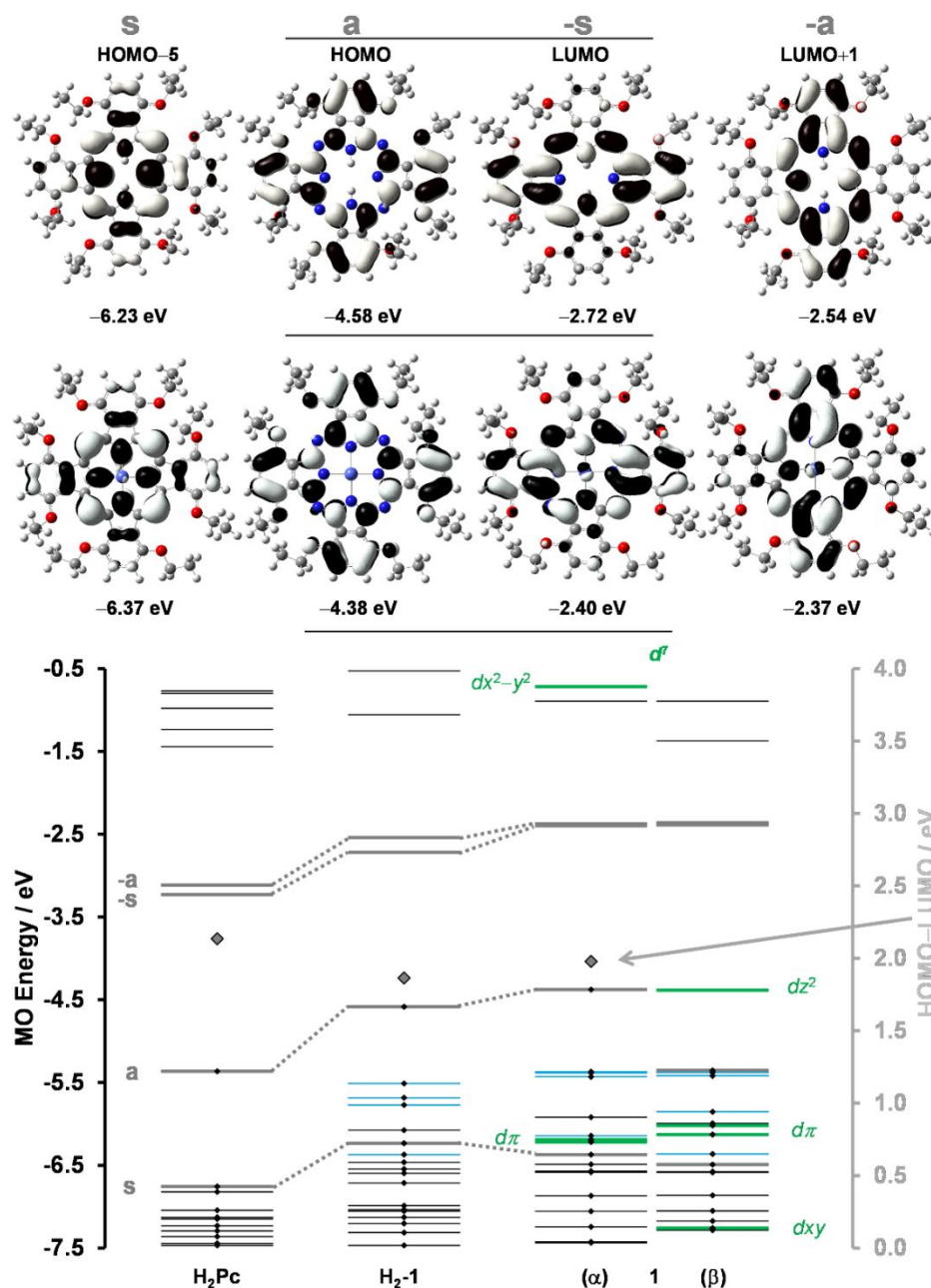


Fig. 2. Angular nodal patterns of the **a**, **s**, **-a** and **-s** MOs of **H₂-1** (TOP) and **1** (CENTER) at an isosurface value of 0.02 a.u. MO energies (BOTTOM) of the parent non-metallated phthalocyanine with no peripheral substituents (**H₂Pc**), **1** and its non-metallated precursor (**H₂-1**) at the B3LYP/SDD level of theory (bottom). The occupied MOs are highlighted with black diamonds. The **a**, **s**, **-a** and **-s** MOs are highlighted with thicker gray lines, while green lines denote MOs that are largely associated with the 3*d* atomic orbitals of the Co(II) ion. Blue lines denote π -MOs that have large MO coefficients on the peripheral fused benzene rings, and hence are most likely to be destabilized through a mesomeric interaction with the electron-donating alkoxy substituents. The HOMO-LUMO gaps are plotted against a secondary axis and are highlighted with gray diamonds.

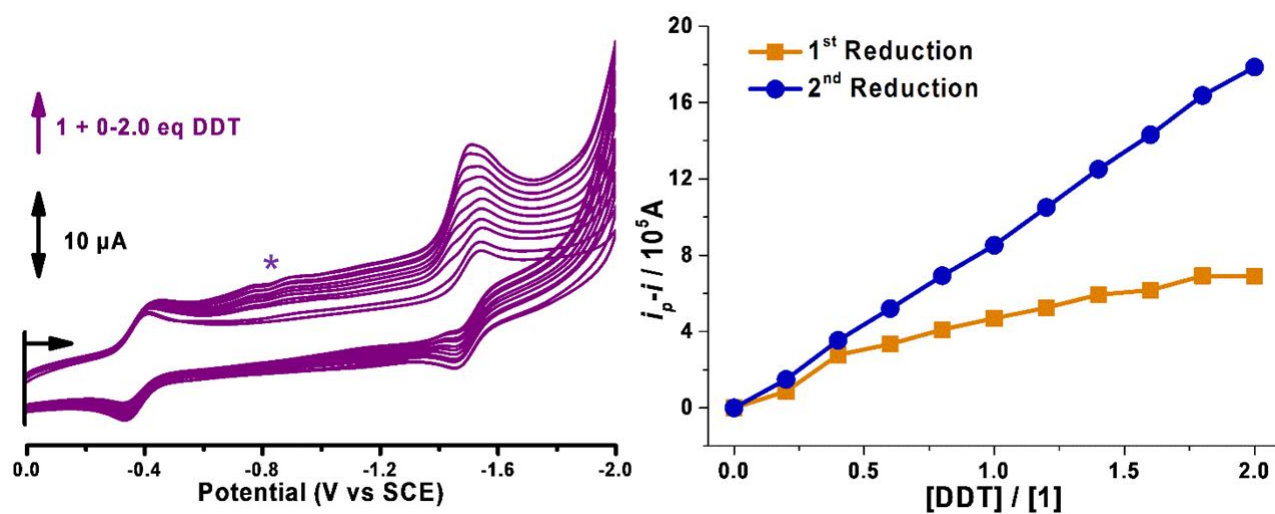


Fig. 3. Left: Reductive electrochemical measurements for **1** upon addition of 0.0–2.0 eq of DDT in DMF containing 0.1 M TBAP. Additional irreversible reduction peaks are observed following the addition of DDT that are indicated with an asterisk. Right: Plots of $i_p - i$ vs. the ratio of [DDT]/[**1**] in DMF containing 0.1 M TBAP.

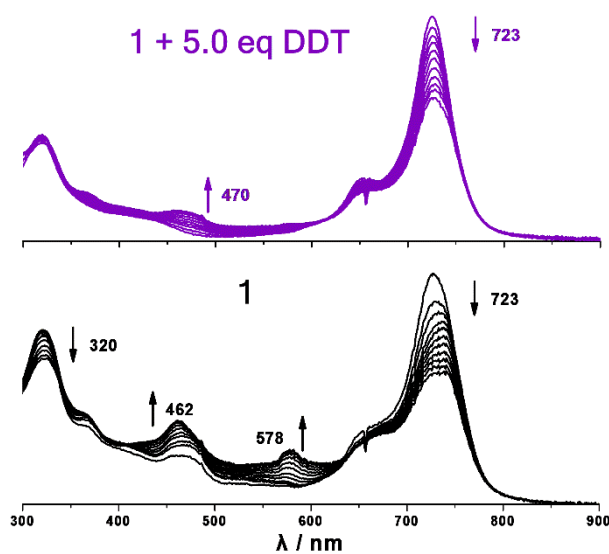


Fig. 4. Reductive spectroelectrochemical measurement for **1** at an applied potential at $E = -1.85$ V in the presence (top) or absence (bottom) of DDT in DMF containing 0.1 M TBAP.

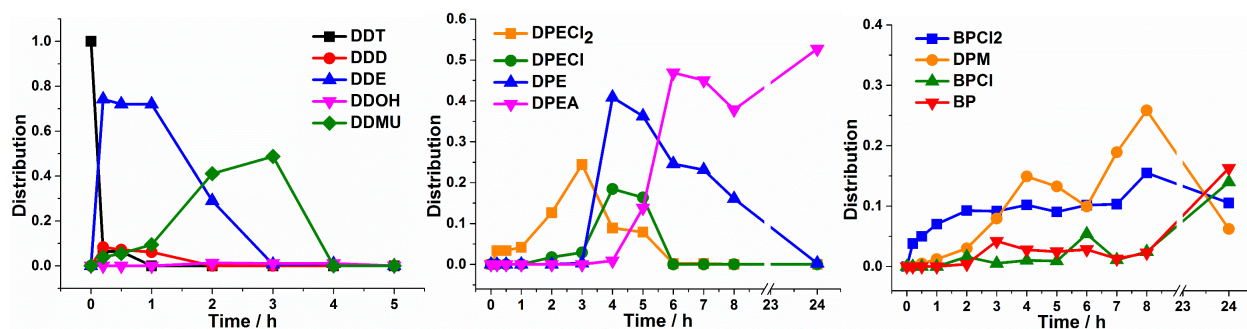


Fig. 5. The time-dependent distribution of DDT and its electrocatalyzed C-Cl bond cleavage products identified by GC during controlled-potential electrolysis with **1** at $E = -1.85$ V in DMF containing 0.1 M TBAP.

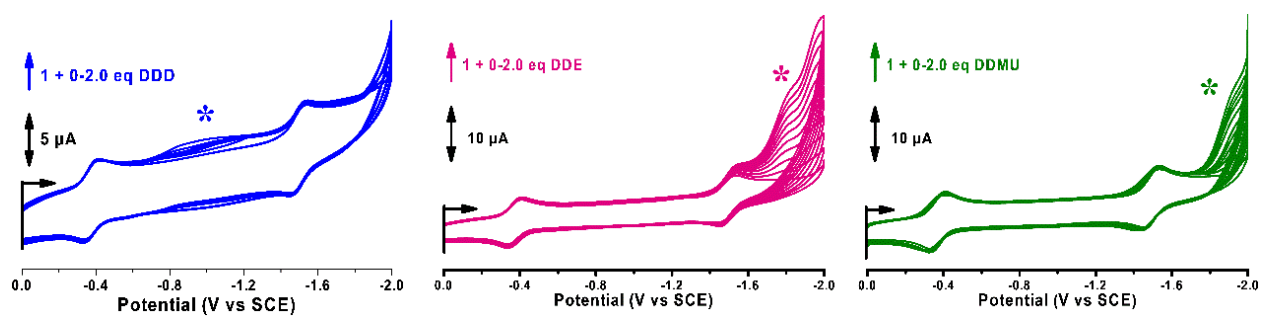


Fig. 6. Reductive cyclic voltammetry measurements for **1** in the presence of 0.0–2.0 eq of DDD (left), DDE (middle) and DDMU (right) in DMF containing 0.1 M TBAP. Additional irreversible reduction peaks are observed following the addition of DDT and these are indicated by asterisks.

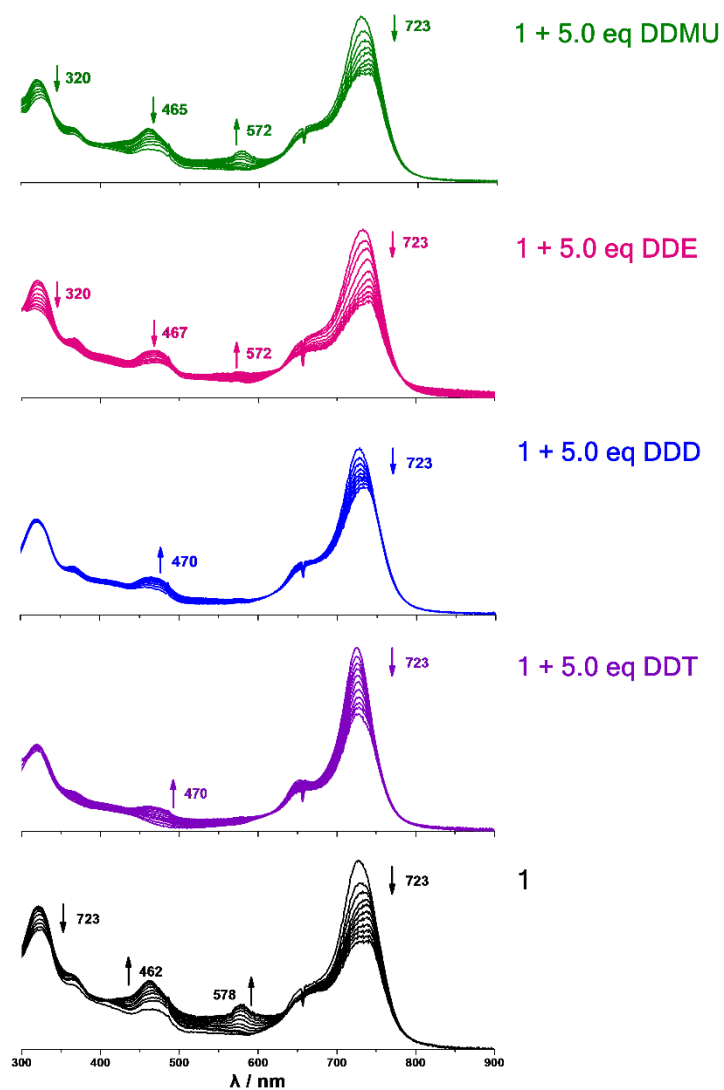


Fig. 7. *In situ* spectroelectrochemistry of **1** in the absence and presence of 5.0 eq of DDT (purple), DDD (blue), DDE (pink) and DDMU (green) in DMF containing 0.1 M TBAP.

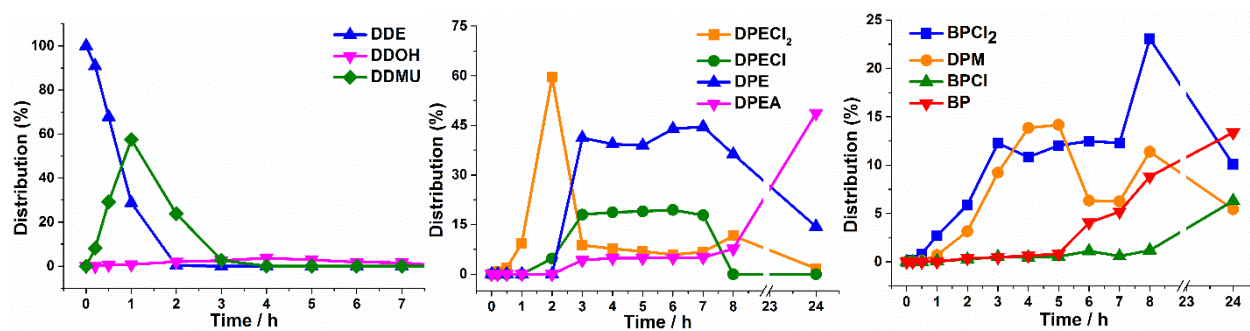


Fig. 8. The time-dependent distribution of DDE and its electrocatalyzed C–Cl bond cleavage products identified by GC during controlled-potential electrolysis with **1** at $E = -1.85$ V in DMF containing 0.1 M TBAP.

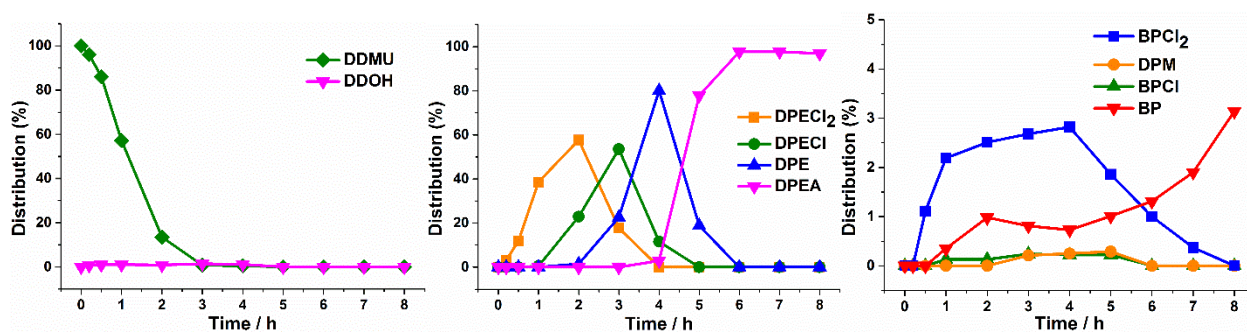


Fig. 9. The time-dependent distribution of DDMU and its electrocatalyzed C-Cl bond cleavage products identified by GC during controlled-potential electrolysis with **1** at $E = -1.85$ V in DMF containing 0.1 M TBAP.

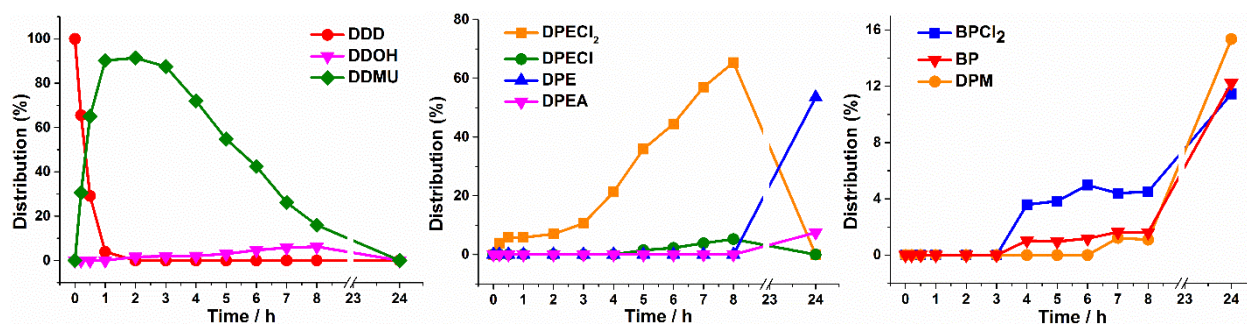


Fig. 10. The time-dependent distribution of DDD and its electrocatalyzed C–Cl bond cleavage products identified by GC during controlled-potential electrolysis with **1** at $E = -1.85$ V in DMF containing 0.1 M TBAP.